TTP95-42
MADPH-95-916
November 1995

Dijet Production at HERA in Next-to-Leading Order

Erwin Mirkes[a] and Dieter Zeppenfeld[b]

[a] *Institut für Theoretische Teilchenphysik, Universität Karlsruhe, D-76128 Karlsruhe, Germany*

[b] *Department of Physics, University of Wisconsin, Madison, WI 53706, USA*

Abstract

Two-jet cross sections in deep inelastic scattering at HERA are calculated in next-to-leading order. The QCD corrections are implemented in a new $ep \to n$ jets event generator, MEPJET, which allows to analyze arbitrary jet definition schemes and general cuts in terms of parton 4-momenta. First results are presented for the JADE, the cone and the k_T schemes. For the W-scheme, disagreement with previous results and large radiative corrections and recombination scheme dependencies are traced to a common origin.

Deep inelastic scattering (DIS) at HERA is a copious source of multi-jet events. Typical two-jet cross sections[1] are in the 100 pb to few nb range and thus provide sufficiently high statistics for precision QCD tests [1,2]. Topics to be studied include the determination of $\alpha_s(\mu_R^2)$ over a wide range of scales, measurement of the gluon structure function (via $\gamma g \to q\bar{q}$), and the study of internal jet structure. Clearly, next-to-leading order (NLO) QCD corrections are mandatory on the theoretical side. The dijet cross section, for example, is proportional to $\alpha_s(\mu_R)$ at leading order (LO), thus suggesting a direct measurement of the strong coupling constant. However, the LO calculation leaves the renormalization scale μ_R undetermined. The NLO corrections substantially reduce the renormalization and factorization scale dependencies which are present in the LO calculations and thus reliable cross section predictions in terms of $\alpha_s(m_Z)$ are made possible. NLO corrections in jet physics imply that a jet (in a given jet definition scheme) may consist of two partons. Thus first sensitivity to the internal jet structure is obtained, like dependence on the cone size or on recombination prescriptions. This will be of particular importance in the subsequent discussion.

In this Letter, we investigate NLO QCD corrections to two-jet production in various jet algorithms at HERA energies. Previous calculations [3–5] were limited to a JADE type algorithm, called W-scheme below. In addition, approximations were made to the matrix elements which, as we will show, are not valid in large regions of phase space. Our calculation uses the s_{min} technique of Giele and Glover [6]. This technique considerably simplifies the structure of NLO QCD corrections to hadronic processes and has already been applied to the calculation of NLO jet cross sections at LEP and the Tevatron [6,7]. The calculation is based on a QED-type factorization of soft gluon singularities [6] and the use of universal "crossing functions" [7]. This allows for a modular approach to NLO calculations. Our calculation of dijet production in DIS is implemented as a full NLO Monte Carlo program, MEPJET. The essential benefit of the Monte Carlo approach [8] is that all hard phase space integrals are performed numerically. This makes the implementation of arbitrary cuts and jet algorithms a relatively easy task.

Let us briefly discuss the essential features of our calculation. Further details will be given in a subsequent publication. Deep inelastic electron proton scattering with several partons in the final state,

$$e^-(l) + p(P) \to e^-(l') + \text{proton remnant}(p_r) + \text{parton } 1(p_1) + \ldots + \text{parton } n(p_n) \qquad (1)$$

proceeds via the exchange of an intermediate vector boson $V = \gamma, Z$. In the following, Z-exchange will be neglected. We denote the momentum of the virtual photon, γ^*, by $q = l - l'$, its absolute square by Q^2, the square of the final hadronic mass by $W^2 = (P+q)^2$ and use the standard scaling variables $x = Q^2/(2P \cdot q)$ and $y = P \cdot q / P \cdot l$. The general structure of the n-jet cross section in DIS is given by

$$d\sigma^{had}[n-\text{jet}] = \sum_a \int d\eta \; f_a(\eta, \mu_F^2) \; d\hat{\sigma}^a(p = \eta P, \alpha_s(\mu_R^2), \mu_R^2, \mu_F^2) \qquad (2)$$

[1]In the following the jet due to the beam remnant is not included in the number of jets.

where the sum runs over incident partons $a = q, \bar{q}, g$ which carry a fraction η of the proton momentum. $\hat{\sigma}^a$ denotes the partonic cross section from which collinear initial state singularities have been factorized out at a scale μ_F and implicitly included in the scale dependent parton densities $f_a(\eta, \mu_F^2)$. In Born approximation, the subprocesses $\gamma^* + q \to q + g$, $\gamma^* + \bar{q} \to \bar{q} + g$, and $\gamma^* + g \to q + \bar{q}$ contribute to the two-jet cross section. At $\mathcal{O}(\alpha_s^2)$ the real emission corrections involve $\gamma^* + q \to q + g + g$, $\gamma^* + q \to q + \bar{q} + q$, $\gamma^* + g \to q + \bar{q} + g$ and analogous anti-quark initiated processes. The corresponding cross sections are calculated by numerically evaluating the tree level helicity amplitudes as given in Ref. [9]. Similarly, the finite parts of the one-loop amplitudes are obtained by crossing the one-loop results for $e^+e^- \to q\bar{q}g$ from Ref. [6]. The numerical evaluation of helicity amplitudes has the advantage that the full spin structure is kept and, therefore, the MEPJET program allows for the calculation of all possible jet-jet and jet lepton correlations in NLO. In addition the NLO corrections for polarized electron on polarized proton scattering [10] become available.

In the one-loop amplitudes the ultraviolet divergencies are removed by $\overline{MS}$ renormalization which introduces a dependence on the renormalization scale μ_R. Infrared as well as collinear divergencies associated with the final state partons are cancelled against corresponding divergencies of the one-loop contributions (see below). The remaining collinear initial state divergencies are factorized into the bare parton densities introducing a dependence on the factorization scale μ_F. In order to handle these singularities we follow Ref. [7] and use the technique of universal "crossing functions". Starting from the results of the NLO calculation with all partons in the final state, *i.e.* $e^+e^- \to n + 1$ jets, where no such singularities occur after adding real and virtual contributions, the "crossing functions" contain the convolutions of the parton distribution functions with Altarelli-Parisi kernels and in addition take into account the crossing of a final state cluster to the intitial state, within the s_{min} cone as defined below. Note that all "plus" prescriptions are absorbed into the numerical evaluation of these crossing functions.

The 3-parton final states need to be integrated over the entire phase space, including the unresolved regions, where only two jets are reconstructed according to a given jet definition scheme. In order to isolate the infrared as well as collinear divergencies associated with these unresolved regions the resolution parameter s_{min} is introduced. Soft and collinear approximations are used in the region where at least one pair of partons, including initial ones, has $s_{ij} = 2p_i \cdot p_j < s_{min}$ and the soft and/or collinear final state parton is integrated over analytically. Adding this soft+collinear part to the virtual contributions gives a finite result for, effectively, 2-parton final states. In general this 2-parton contribution is negative and grows logarithmically in magnitude as s_{min} is decreased. This logarithmic growth is exactly cancelled by the increase in the 3 parton cross section, once s_{min} is small enough for the approximations to be valid. The integration over the 3-parton phase space with $s_{ij} > s_{min}$ is done by Monte-Carlo techniques (without using any approximations). Since, at each phase space point, the parton 4-momenta are available, the program is flexible enough to implement any jet definition algorithms or to impose arbitrary kinematical resolution and acceptance cuts on the final state particles. This is an essential advantage over existing programs such as DISJET [5].

A powerful test of the numerical program is the s_{min} independence of the final result. Fig. 1 shows the inclusive dijet cross section as a function of s_{min} for the jet algorithms to be defined below. As mentioned before, s_{min} is an arbitrary theoretical parameter and

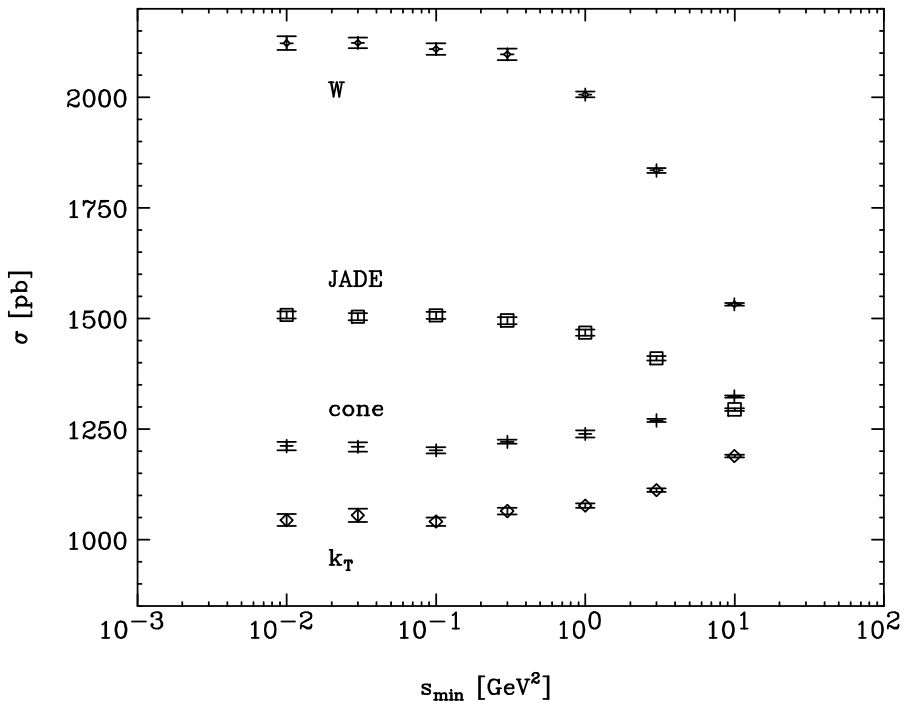

FIG. 1. Dependence of the inclusive two-jet cross section in the k_T, cone, JADE, and the W-scheme on s_{min}, the two-parton resolution parameter. Partons are recombined in the E-scheme. Error bars represent statistical errors of the Monte Carlo program. For the fairly soft jet definition criteria described in the text, s_{min} independence is achieved for $s_{min} \lesssim 0.1$ GeV^2.

any measurable quantity should not depend on it. One observes that for values smaller than 0.1 GeV^2 the results are indeed independent of s_{min}. The strong s_{min} dependence of the NLO cross sections for larger values shows that the soft and collinear approximations used in the phase space region $s_{ij} < s_{min}$ are no longer valid, *i.e.* terms of $\mathcal{O}(s_{min})$ and $\mathcal{O}(s_{min} \ln s_{min})$ become important. In general, one wants to choose s_{min} as large as possible to avoid large cancellations between the virtual+collinear+soft part ($s_{ij} < s_{min}$) and the hard part of the phase space ($s_{ij} > s_{min}$). Note that factor 10 cancellations occur between the effective 2-parton and 3-parton final states at the lowest s_{min} values in Fig. 1 and hence very high Monte Carlo statistics is required for these points. s_{min} independence is achieved at and below $s_{min} = 0.1$ GeV^2 and we choose this value for our further studies.

For these numerical studies, the standard set of parton distribution functions is MRS set D-' [11]. We employ the two loop formula for the strong coupling constant with $\Lambda^{(4)}_{\overline{MS}} = 230$ MeV, which is the value from the parton distribution functions. The value of α_s is matched at the thresholds $\mu_R = m_q$ and the number of flavors is fixed to $n_f = 5$ throughout, *i.e.* gluons are allowed to split into five flavors of massless quarks. Unless stated otherwise, the renormalization scale and the factorization scale are set to $\mu_R = \mu_F = 1/2 \sum_i p_T^B(i)$, where $p_T^B(i)$ denotes the magnitude of the transverse momentum of parton i in the Breit

TABLE I. Two-jet cross sections in DIS at HERA. Results are given at LO and NLO for the four jet definition schemes and acceptance cuts described in the text.

	two-jet LO	two-jet exclusive NLO	two-jet inclusive NLO
cone	1107 pb	1047 pb	1203 pb
k_T	1067 pb	946 pb	1038 pb
W	1020 pb	2061 pb	2082 pb
JADE	1020 pb	1473 pb	1507 pb

frame. A running QED fine structure constant $\alpha(Q^2)$ is used. The lepton and hadron beam energies are 27.5 and 820 GeV, respectively. A minimal set of kinematical cuts is imposed on the initial virtual photon and on the final state electron and jets. We require $40\ \mathrm{GeV}^2 < Q^2 < 2500\ \mathrm{GeV}^2$, $0.04 < y < 1$, an energy cut of $E(e') > 10$ GeV on the scattered electron, and a cut on the pseudo-rapidity $\eta = -\ln\tan(\theta/2)$ of the scattered lepton and jets of $|\eta| < 3.5$. In addition jets must have transverse momenta of at least 2 GeV in both the lab and the Breit frame.

Within these general cuts four different jet definition schemes are considered for which we have chosen parameters such as to give similar LO cross sections (see Table I). In the W-scheme the invariant mass squared $s_{ij} = (p_i + p_j)^2$ is calculated for each pair of final state particles (including the proton remnant). If the pair with the smallest invariant mass squared is below $y_{cut}W^2$, the pair is clustered according to a recombination scheme. Unless stated otherwise, and for all jet algorithms, we use the E-scheme to recombine partons, i.e. the cluster momentum is taken as $p_i + p_j$. This process is repeated until all invariant masses are above $y_{cut}W^2$. The resolution parameter y_{cut} is fixed to 0.02.

The experimental analyses in [1,2] are based on a variant of the W-scheme, the "JADE" algorithm. It is obtained from the W-scheme by replacing the invariant definition $s_{ij} = (p_i + p_j)^2$ by $M_{ij}^2 = 2E_iE_j(1 - \cos\theta_{ij})$, where all quantities are defined in the laboratory frame. Neglecting the explicit mass terms p_i^2 and p_j^2 in the definition of M_{ij}^2 causes substantial differences in jet cross sections between the W and the JADE scheme.

In the cone algorithm (which is defined in the laboratory frame) the distance $\Delta R = \sqrt{(\Delta\eta)^2 + (\Delta\phi)^2}$ between two partons decides whether they should be recombined to a single jet. Here the variables are the pseudo-rapidity η and the azimuthal angle ϕ. We recombine partons with $\Delta R < 1$. Furthermore, a cut on the jet transverse momenta of $p_T(j) > 5$ GeV in the lab frame is imposed in addition to the 2 GeV Breit frame cut.

For the k_T algorithm (which is implemented in the Breit frame), we follow the description introduced in Ref. [12]. The hard scattering scale E_T^2 is fixed to 40 GeV^2 and $y_{cut} = 1$ is the resolution parameter for resolving the macro-jets. In addition, jets are required to have a minimal transverse momentum of 5 GeV in the Breit frame.

With these parameters, one obtains the two-jet cross sections of Table I. While the higher order corrections in the cone and k_T schemes are small, very large corrections appear in the W-scheme. In addition, the large effective K-factor (defined as $K = \sigma_{NLO}/\sigma_{LO}$) of 2.04 (2.02) for the two-jet inclusive (exclusive) cross section in the W-scheme depends strongly on the recombination scheme which is used in the clustering algorithm (see below).

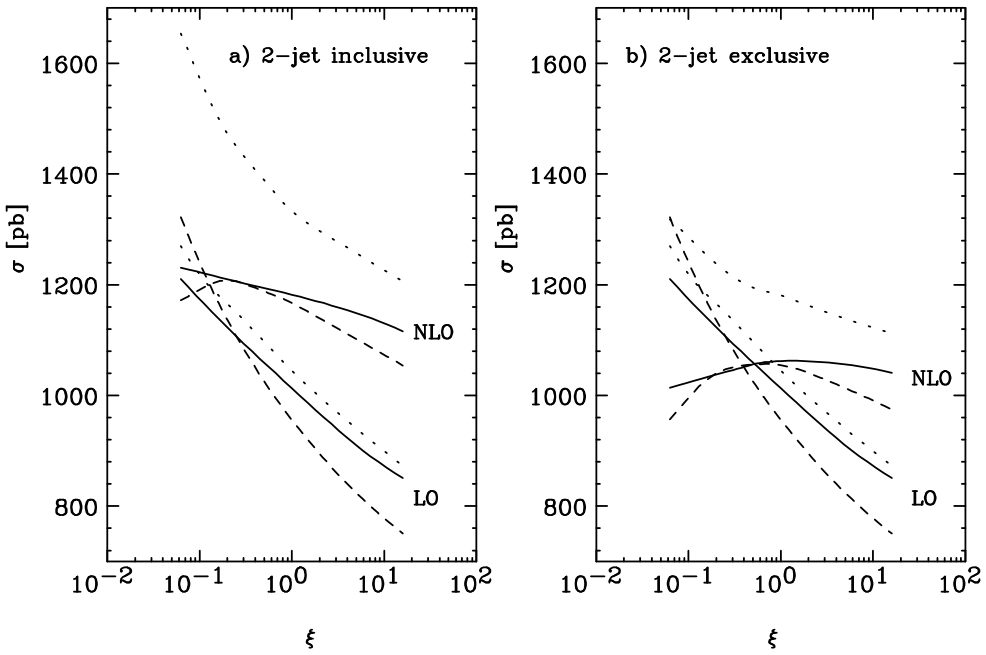

FIG. 2. Dependence of a) the two-jet inclusive and b) the two-jet exclusive cross section in the cone scheme on the renormalization and factorization scale factor ξ. The solid curves are for $\mu_R^2 = \mu_F^2 = \xi\,(\sum_i\, p_T^B(i))^2$, while for the dashed curves only $\xi_R = \xi$ is varied but $\xi_F = 1/4$ is fixed. Choosing the photon virtuality as the basic scale yields the dotted curves, which correspond to $\mu_R^2 = \mu_F^2 = \xi\, Q^2$. Results are shown for the LO (lower curves) and NLO calculations.

A good measure of the improvement at NLO is provided by the residual scale dependence of the cross section. We have considered scales related to the scalar sum of the parton transverse momenta in the Breit frame, $\sum_i\, p_T^B(i)$, and the virtuality Q^2 of the incident photon. In Fig. 2 the dependence of the two-jet cross section, in the cone scheme, on the renormalization and factorization scale factors ξ_R and ξ_F is shown. For scales related to $\sum_i\, p_T^B(i)$ they are defined via

$$\mu_R^2 = \xi_R\,(\sum_i\, p_T^B(i))^2\,, \qquad \mu_F^2 = \xi_F\,(\sum_i\, p_T^B(i))^2\,. \tag{3}$$

For the two-jet inclusive cross section of Fig. 2a, the LO variation by a factor 1.43 is reduced to a 10% variation at NLO when both scales are varied simultaneously over the plotted range (solid curves). However, neither the LO nor the NLO curves show an extremum. The uncertainty from the variation of both scales for the NLO two-jet exclusive cross section in Fig. 2b (solid curves) is reduced to 5%. Furthermore, the two-jet exclusive cross section now has a maximum and is equal to the LO cross section for $\xi = 0.5$. Also shown is the $\xi = \xi_R$ dependence of LO and NLO cross sections at fixed $\xi_F = 1/4$ (dashed curves). In this case a maximum appears in the NLO inclusive and exclusive cross sections. However, the scale variation is stronger than in the $\xi = \xi_R = \xi_F$ case.

An alternative scale choice might be $\mu_R^2 = \mu_F^2 = \xi\, Q^2$. The resulting ξ dependence is shown as the dotted lines for both the LO and NLO calculations. At LO the two scale choices give qualitatively similar results. However, with $\mu_R^2 = \mu_F^2 = \xi\, Q^2$, the scale dependence does

not markedly improve at NLO. In addition a sizable K-factor is found, with $K > 1$ for small values of Q^2 and $K < 1$ for very hard incident photons. We therefore use the jet transverse momenta in the Breit frame to set the scale and fix $\xi_R = \xi_F = 1/4$ in Eq. (3). A further discussion of the scale dependence of dijet cross sections at HERA can be found in Ref. [13].

The effective K-factors close to unity which are found in the cone and k_T schemes could, in principle, be a coincidence arising from compensating effects in different phase space regions. It is important, therefore, to also compare LO and NLO distributions, in particular for those variables which define the acceptance region.

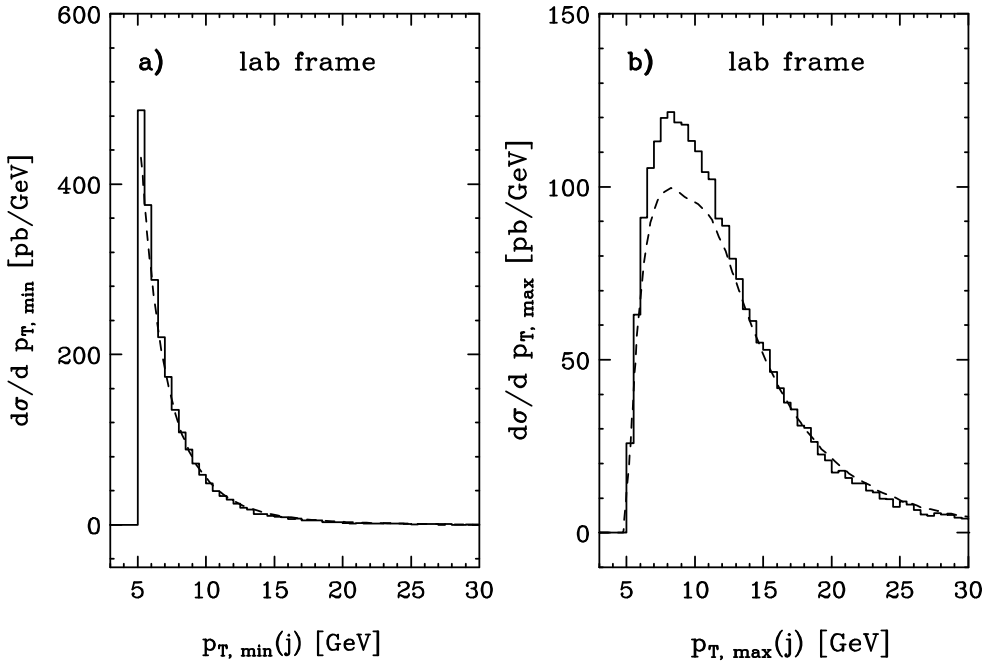

FIG. 3. Transverse momentum distribution in the lab frame for the jet with (a) minimal and (b) maximal transverse momentum. Results are shown for the two-jet inclusive cross section in the cone scheme in leading (dashed curves) and next-to-leading order (histograms).

The transverse momentum distributions of the softest and the hardest jet in the laboratory frame are shown in Fig. 3, for the cone scheme. The fairly small NLO corrections allow for reliable theoretical predictions. In general the largest radiative corrections are observed at small jet p_T, as evidenced by the shape change in the $p_{T,max}$ distribution of Fig. 3b. The predictions are therefore expected to become more reliable for higher jet transverse momenta. A potential problem is the very steep $p^{lab}_{T,min}$ distribution, which, via the cut at 5 GeV, introduces a strong sensitivity to the correct matching of the parton p_T and the measured jet p_T. However, this is a general problem for all jet algorithms, *i.e.* the jet rate falls very rapidly as the required energy scale of the jets is increased.

A more critical case is shown in Fig. 4 where, for jets defined in the k_T-scheme, the jet rapidity and the electron transverse momentum in the lab frame are shown. At NLO jets are produced somewhat more forward (in the proton direction) than at LO, see Fig. 4a. Hence, the rapidity cut at $|\eta_j| = 3.5$ has a stronger effect in NLO, which partially explains the relatively low K-factor of 0.97 in the k_T-scheme.

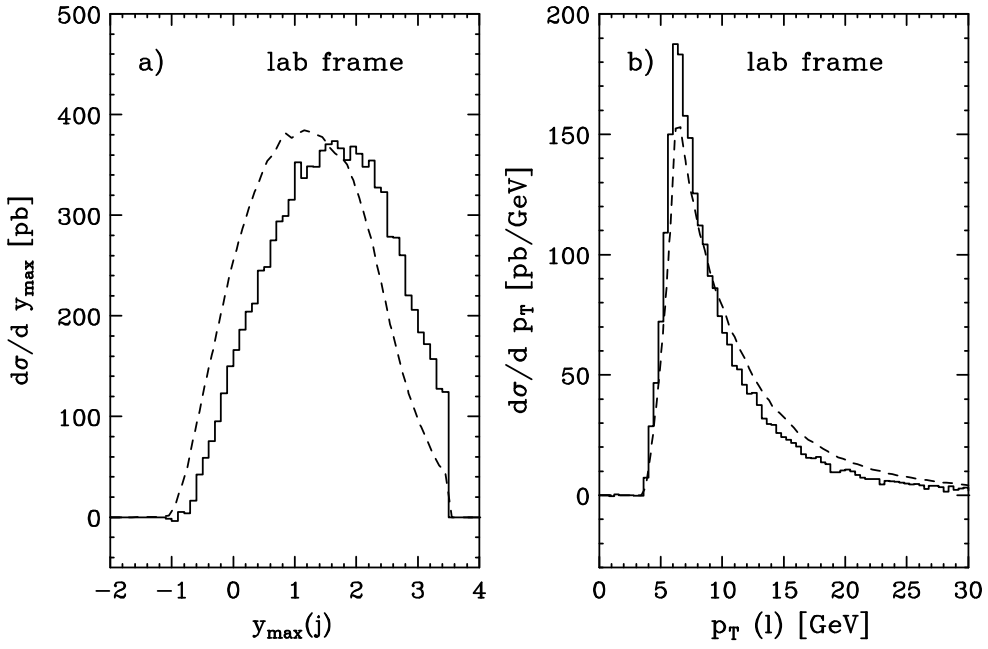

FIG. 4. Rapidity distribution of the most forward jet (a) and transverse momentum distribution of the scattered electron (b) in the lab frame. Results are shown for the k_T scheme in leading (dashed curves) and next-to-leading order (histograms) for the two-jet inclusive cross section.

Another observable which exhibits rather large NLO corrections is the electron transverse momentum distribution in Fig. 4b. The electron p_T becomes considerably softer at NLO, with an effective K-factor above unity at small $p_T(\ell)$ and $K < 1$ in the high transverse momentum region. In view of these shape changes the overall small change at NLO has to be considered a coincidence, tied to the choice of $p_T(\ell)$ range. Since the electron transverse momentum and the Q^2 of the event are very closely related, a similar change in the size of radiative corrections is obtained by choosing different Q^2 bins. Very similar effects on the $y_{max}(j)$ and $p_T(l)$ distributions are also observed in the other jet definition schemes. As a result, a judicious choice of phase space region could generate very large or small K-factors which would indicate that, in these phase space regions, even the NLO calculation is fraught with large uncertainties. To avoid such potential problems, one should investigate the effect of the higher order corrections on those variables which are used to define kinematical cuts.

A somewhat disturbing result of our calculation is the surprisingly large effective K-factor in the W-scheme, in particular since we disagree here with previous calculations [2] [4,5]. The DISJET program [5], for example, gives a K-factor very close to unity for a phase space region which is very similar[3] to the one considered above. The main difference to these earlier

[2]About 10% are explained by differences in the virtual results for the "longitudinal projection" in the first paper of [4]. This has been corrected in the latest version of [5].

[3] The DISJET program does not allow to impose exactly the same kinematical cuts as discussed

calculations is the treatment of partons which are recombined into a jet. Previously, collinear and soft approximations were made for all partons which are coalesced into a single jet, *i.e.* for any pair of final state particles (including the remnant) with $s_{ij} < y_{cut}\ W^2$, neglecting terms of order $y_{cut}W^2$. In our calculation, similar [4] approximations are only made in a much smaller region, $s_{ij} < s_{min}$ for any pair of initial and final state partons, and we are able to study the small s_{min} limit. Effectively, the approximations in Refs. [4,5] correspond to the replacement of a massive two-parton system by a single massless jet. How well justified are these approximations?

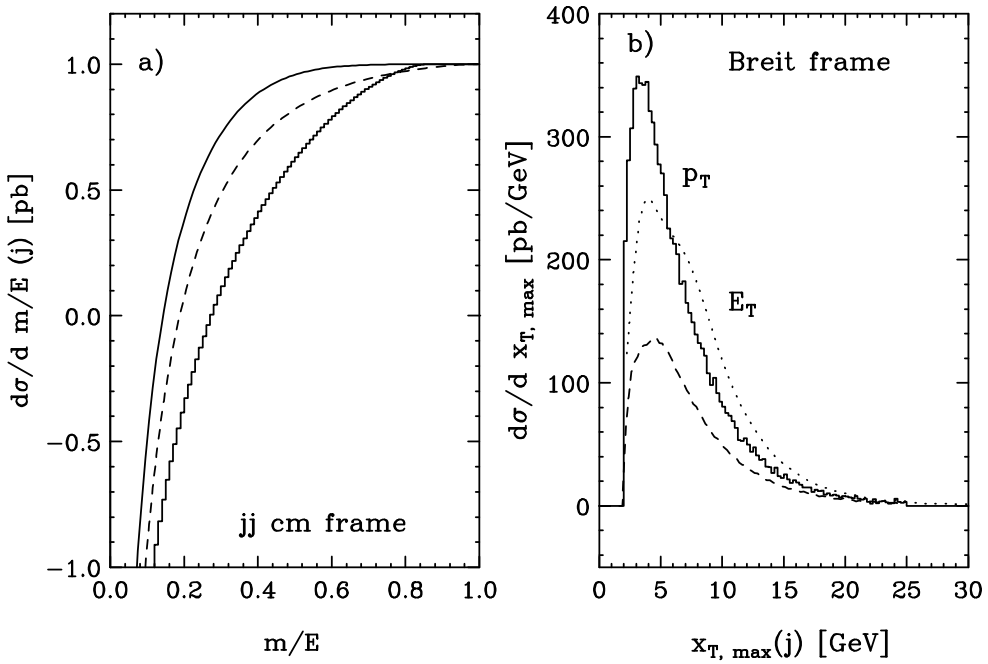

FIG. 5. Single jet mass effects at next-to-leading order. (a) Fraction of events in the cone scheme (solid curve), k_T scheme (dashed curve), and W-scheme (histogram) with all jet mass to energy ratios below m/E, where E is the corresponding jet's energy in the parton center of mass frame. Negative values at small m/E are due to virtual contributions at $m/E = 0$. (b) Next-to-leading order transverse momentum ($x_T = p_T$, solid histogram) and transverse-energy distribution ($x_T = E_T$, dotted curve) for the jet with largest p_T and E_T in the Breit frame, for the W-scheme. The dashed curve shows the leading order result where both distributions are identical.

In Fig. 5a the fraction of events is shown with at least one jet being more massive than m/E. Here m is the invariant mass and E the energy of the most massive of the jets in the parton center of mass frame. In LO $m/E \equiv 0$ since we are always using massless partons. At

---

before for the W-scheme; however, this is not relevant for the argument.

[4]Our approximations in the soft and collinear region are stronger than the approximations made in [4,5] where, effectively, also terms proportional to $s_{ij} \ln s_{ij}$ are kept. These latter terms are neglected here.

NLO the median m/E is 0.44 in the W-scheme (*i.e.* 50% of the NLO cross section lies in the range $m/E > 0.44$), while substantially smaller values, 0.30 and 0.22 are found in the k_T and cone schemes. The large single jet masses (compared to their energy) imply that collinear or soft approximations for the partons inside a NLO jet are not generally permissable. Indeed the slow approach to the asymptotic region visible in Fig. 1 shows that only for two parton invariant masses squared $s_{ij} \lesssim 0.1$ GeV^2 are such approximations allowed. It is these mass effects which were not treated correctly in previous calculations.

The very large median value of m/E in the W-scheme implies that at NLO we are dealing with very different types of jets than at LO. At NLO at least one of the W-scheme jets extends over a large solid angle, it is a massive, slow moving object in the center of mass frame and, hence, very different from the pencil-like, massless objects called jets at LO. The typically small relativistic γ-factor of these jets has large kinematic effects. For example the difference between transverse energy and transverse momentum distributions of the jets, which are shown in Fig. 5b, becomes quite pronounced in the W-scheme, an effect which is much smaller in the k_T and cone schemes.

The fact that very different kinematical regions are populated by the LO and NLO jets implies that radiative corrections may be very large as is indeed indicated by the large effective K-factor in the W-scheme. The large corrections in turn imply that the predicted jet cross sections have large theoretical uncertainties and should not be used for precise QCD tests. Another measure of these uncertainties is the recombination scheme dependence of the predicted two-jet inclusive cross section. In the $E0$ and P-schemes, where two partons are recombined to a massless jet, K is reduced to 1.41 and 1.29, respectively. This dependence first appears in the NLO calculation, where a jet may be composed of two partons. This internal jet structure, however, is only simulated at tree level and thus the dependence of the cross section on the recombination scheme is subject to potentially large higher order corrections.

These uncertainties are small for jet algorithms with small recombination scheme dependence. In the JADE-algorithm the K-factor is reduced from 1.48 in the E-scheme to 1.36 and 1.24 in the $E0$ and P-schemes. For the cone (k_T) scheme this recombination scheme dependence is reduced to the 3% (10%) level. The K-factor close to unity as well as this small recombination scheme dependence indicate that theoretical uncertainties due to higher order corrections are fairly small in the cone and k_T scheme, and both schemes appear to be well suited for QCD studies at HERA.

ACKNOWLEDGMENTS

D. Z. would like to thank the CERN theory group, where part of this work was completed, for its hospitality. E. M. is happy to acknowledge many stimulating conversations with the ZEUS collaboration and in particular with B. Musgrave, S. Magill, I. Park, J. Repond and T. Trefzger. This research was supported by the University of Wisconsin Research Committee with funds granted by the Wisconsin Alumni Research Foundation and by the U. S. Department of Energy under Grant No. DE-FG02-95ER40896. The work of E. M. was supported in part by DFG Contract Ku 502/5-1.

REFERENCES

[1] H1 Collaboration, T. Ahmed et. al., Phys. Lett. **B346** (1995) 415.
[2] ZEUS Collaboration, M. Derrick et al., DESY-95-182, Oct 1995, hep-ex/9510001.
[3] J.G. Körner, E. Mirkes and G. Schuler, Int. J. Mod. Phys. **A4** (1989) 1781;
T. Brodkorb, J.G. Körner, E. Mirkes, and G. Schuler, Z. Phys. **C44** (1989) 415.
[4] T. Brodkorb and J.G. Körner, Z. Phys. **C54** (1992) 519;
T. Brodkorb and E. Mirkes, Z. Phys. **C66** (1995) 141;
D. Graudenz Phys. Lett. **B256** (1992) 518; Phys. Rev. **D49** (1994) 3291.
[5] T. Brodkorb and E. Mirkes, Madison preprint, MAD/PH/821 (1994).
[6] W. T. Giele and E. W. N. Glover, Phys. Rev. D **46** (1992) 1980.
[7] W. T. Giele, E. W. N. Glover and D.A. Kosower, Nucl. Phys. **B403** (1993) 633.
[8] H. Baer, J. Ohnemus, and J. F. Owens, Phys. Rev. **D40** (1989) 2844; Phys. Lett. **B234** (1990) 127; Phys. Rev. **D42** (1990) 61.
[9] K. Hagiwara and D. Zeppenfeld, Nucl. Phys. **B313** (1989) 560.
[10] C. Ziegler and E. Mirkes, Nucl. Phys. **B429** (1994) 93.
[11] A.D. Martin, W.J. Stirling and R.G. Roberts, Phys. Lett. **B306** (1993) 145.
[12] S. Catani, Y.L. Dokshitzer and B.R. Webber, Phys. Lett. **B285** (1992) 291.
[13] G. Ingelman and J. Rathsman, Z. Phys. **C63** (1994) 589.